SYNTHESIS AND CRYSTAL STRUCTURE OF LiTb$_6$O$_5$(BO$_3$)$_3$

R. E. Nikolaev[1], M. S. Tarasenko[1]*,
N. V. Kuratieva[1], V. A. Trifonov[1],
and N. G. Naumov[1]**

Single crystals of compound LiTb$_6$O$_5$(BO$_3$)$_3$ suitable for X-ray diffraction are prepared by the flux growth method. The compound crystallizes in the $P2_1/n$ space group, $a = 8.4350$ Å, $b = 15.6232$ Å, $c = 8.9025$ Å, $\beta = 92.041°$. The obtained compound belongs to the class of 3D-framework oxoborates. It has a similar structure to that of known LiGd$_6$O$_5$(BO$_3$)$_3$ but is not isostructural to the latter. Both structures are derivatives of fluorite, the predecessor compound in this structural series. The cationic part of the predecessor's structural type is filled by Tb^{3+} and Li$^+$ cations, while its anionic part is formed by oxide ions and oxygen atoms of borate anions. The melting point (1375±15 °C) and the band gap (4 eV) are determined for LiTb$_6$O$_5$(BO$_3$)$_3$.

INTRODUCTION

Crystals, ceramics, and glasses of Tb^{3+} containing compounds are widely studied as magneto-optical media (Faraday isolators). One crucial characteristic of these isolators is the Verdet constant which almost directly depends on the magnetoactive ion concentration in the optical medium. Even though compounds with cubic crystal structures are most often considered as Faraday isolators, magnetoactive media with other types of crystal lattices may be also of interest [1].

Borate compounds attract the attention of researchers primarily as nonlinear optical (NLO) materials [2-4], scintillators [5-7], and phosphors [8]. Borates demonstrate good chemical stability and can be used to grow high optical quality crystals. Borates can form mixed salts containing more than one cation and more than one anion, e.g., numerous natural borate minerals and artificial compounds. To date, several double oxoborates of rare earth elements have been described: LiRE$_6$O$_5$(BO$_3$)$_3$ (RE = Pr–Tm [9], Y [10]), Li$_2$RE$_5$O$_4$(BO$_3$)$_3$ (RE = Yb, Lu) [11], Na$_3$La$_9$O$_3$(BO$_3$)$_8$ [12, 13], Na$_2$RE$_2$O(BO$_3$)$_2$ (RE = Y, Nd, Er [14], Sm, Eu, Gd [15], Dy, Ho [16]), K$_2$RE$_2$O(BO$_3$)$_2$ (RE = La [17], Pr [18]). Some of them were studied as laser materials [19], phosphors [20-24], and as NLO materials [13, 25].

The structural data are available only for gadolinium [9] and yttrium [10] oxoborate phases with the general formula LiRE$_6$O$_5$(BO$_3$)$_3$. No structural data have been reported so far for LiTb$_6$O$_5$(BO$_3$)$_3$ single crystals. Therefore, the present work is devoted to fill this gap. Also, the melting point was determined and diffuse reflectance spectra were recorded for the polycrystalline samples. The band gap was calculated from the diffuse reflectance spectrum.

[1]Nikolaev Institute of Inorganic Chemistry, Siberian Branch, Russian Academy of Sciences, Novosibirsk, Russia; *tarasen@niic.nsc.ru, **naumov@niic.nsc.ru. Original article submitted July 17, 2020; revised August 10, 2020; accepted August 10, 2020.

EXPERIMENTAL

Synthesis of LiTb$_6$O$_5$(BO$_3$)$_3$. Polycrystalline LiTb$_6$O$_5$(BO$_3$)$_3$ was prepared in air from high purity reagents (Li$_2$CO$_3$, H$_3$BO$_3$, Tb$_4$O$_7$) taken in the stoichiometric ratio. The resulting sample was a single-phase compound which, however, had a brownish color due to a small number of Tb^{4+} ions in the structure. Annealing the sample in hydrogen at 600 °C for 2 h resulted in a white powder of LiTb$_6$O$_5$(BO$_3$)$_3$.

Growth of LiTb$_6$O$_5$(BO$_3$)$_3$ crystals. The crystals were grown from the terbium oxide rich part of the Tb$_2$O$_3$–B$_2$O$_3$–Li$_2$O system using crystallization from a high-temperature solution. The solution was kept in a high-purity argon atmosphere (99.998 vol.%) at 1050 °C for 100 h and then cooled to room temperature at a rate of 85 °C/h. Well-shaped millimeter size crystals were formed on the walls of a platinum crucible and were easily separated from the solidified melt by chipping and washing them in a dilute hydrochloric acid solution.

The melting point was measured using an original setup described in detail in [26]. The setup was calibrated to the melting points of the standards: Cu (1085 °C), Si (1410 °C), and Pd (1555 °C). The heating was carried out in a molybdenum crucible at a rate of 50 deg/s in helium (99.995 vol.%) under a pressure of 2 atm. The melting point of the substance was determined to be 1375±15 °C.

The diffuse reflectance spectra were recorded on a UV/VIS/NIR Shimadzu 3101 PC spectrometer.

X-ray diffraction analysis. The experimental data were obtained on a D8 VENTURE Bruker AXS diffractometer equipped with a (CMOS) PHOTON 100 detector (MoK_α radiation, $\lambda = 0.71073$ Å). The structures were solved by direct methods and refined anisotropically by full-matrix least-squares using the SHELXL package [27]. After the localization of terbium, oxygen, and boron atoms and their anisotropic refinement, a 5.83 e peak (corresponding to lithium) was found in the electron density map at a distance of 2.04-2.58 Å from the oxygen atoms. After the refining the coordinates, the lithium atom Li1 was also refined anisotropically. The crystallographic and diffraction experiment data for compound **1** are listed in the Table 1. The obtained atomic coordinates and thermal parameters were deposited with the Cambridge Crystallographic Data

TABLE 1. Crystal Data and Structure Refinement Details for Compound **1**

Parameter	1
Empirical formula	B$_3$LiO$_{14}$Tb$_6$
Formula weight	1216.89
Crystal system	Monoclinic
Space group	$P2_1/n$
Lattice parameters: a, b, c, Å; β, deg	8.4350(2), 15.6232(3), 8.9025(2); 92.0410(10)
Volume, Å^3	1172.44(4)
Z	4
ρ_{calc}, g/cm^3	6.894
μ, mm^{-1}	35.781
F(000)	2080
Crystal size, mM	0.080×0.070×0.060
θ range for data collection, deg	2.635-28.394
Index ranges	$-11 \leq h \geq 10$, $-20 \leq k \geq 20$, $-11 \leq l \geq 11$
Reflections collected / unique	10035 / 2934
R_{int}	0.0272
T_{max} / T_{min}	0.162 / 0.223
Restraints / parameters	6 / 218
$GOOF$ on F^2	1.179
Final R indices [$I > 2\sigma(I)$]	$R_1 = 0.0176$, $wR_2 = 0.0360$
R indices (all data)	$R_1 = 0.0194$, $wR_2 = 0.0365$
Largest difference peak / hole, e/Å^3	1.186 / -1.259

Centre (**1** CCDC 2010737) and can be requested from the Cambridge Crystallographic Data Centre and the Fachinformationszentrum Karlsruhe Access Structures service at www.ccdc.cam.ac.uk/structures.

Description of the structure. The compound crystallizes in the $P2_1/n$ space group, monoclinic crystal system. The asymmetric part contains 1 lithium atom, 6 terbium atoms, 3 boron atoms, and 14 oxygen atoms. All these atoms occur in general positions (4e).

The compound is a 3D-framework close packed structure. The coordination environment of each terbium atom is formed by the oxygen atoms belonging to isolated oxide ions and those of borate anions. The coordination environment of atoms Tb1–Tb4 is represented by distorted seven-vertex polyhedra with the following interatomic distances: Tb1–O varying from 2.244(3) Å to 2.436(3) Å (av. 2.35(6) Å); Tb2–O varying from 2.222(3) Å to 2.543(4) Å (av. 2.36(12) Å); Tb3–O varying from 2.297(3) Å to 2.428(4) Å (av. 2.35(5) Å); Tb4–O and varying from 2.271(3) Å to 2.437(4) Å (av. 2.36(5) Å). The coordination environment of atoms Tb5 and Tb6 is represented by strongly distorted cubes with distances Tb5–O varying from 2.260(3) Å to 2.833(4) Å (av. 2.46(22) Å) and distances Tb6–O varying from 2.277(3) Å to 3.031(3) Å (av. 2.52(30) Å). The RE–O distance (> 3 Å) is also present in the structure with gadolinium (Gd5–O6 distance is 3.058 Å [9]) and the one with yttrium (Y4–O6 distance is 3.091 Å [10]). The coordination polyhedra of terbium are shown in Fig. 1. The boron and oxygen atoms in the triangular borate anions occur in the same plane, the B–O distances vary in the region of 1.360(6)-1.391(6) Å. The O–B–O angles fall within the region of 117.3(4)-125.0(5)° (av. 120.0(28)°). The borate anions are coordinated to the terbium atoms both in the monodentate and in the bidentate manner (see Fig. 2). In the close packing, all terbium atoms are connected via five oxide anions each having a tetrahedral environment. In this case, through channels
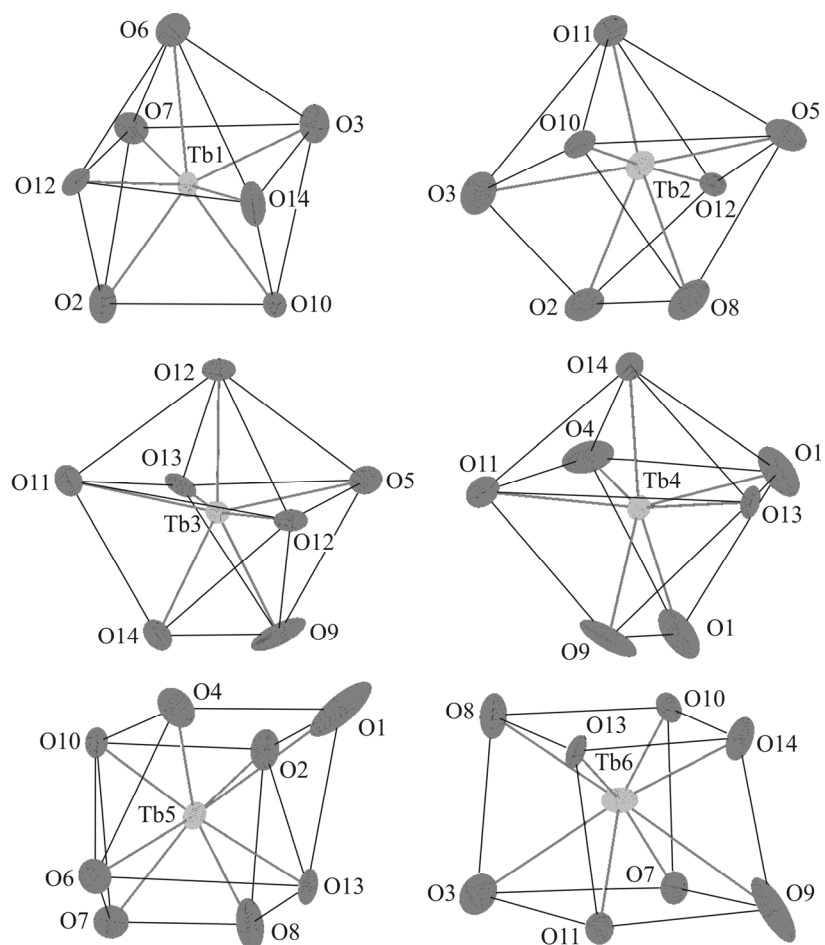

Fig. 1. Coordination environments of terbium atoms (thermal ellipsoids are set at the 95% probability level).
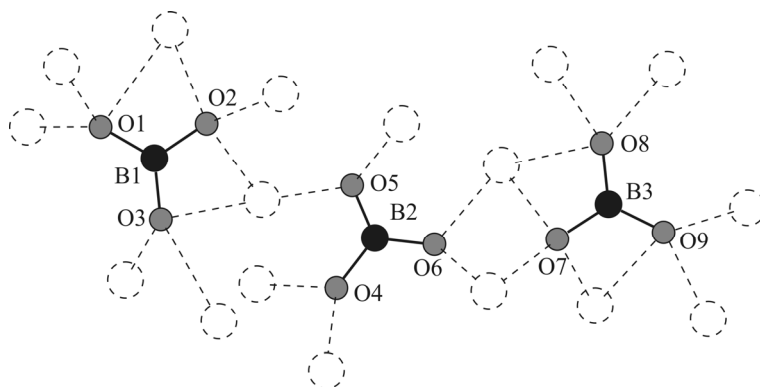
Fig. 2. Coordination of borate anions to the terbium cations. The terbium atoms are shown by dashed lines.
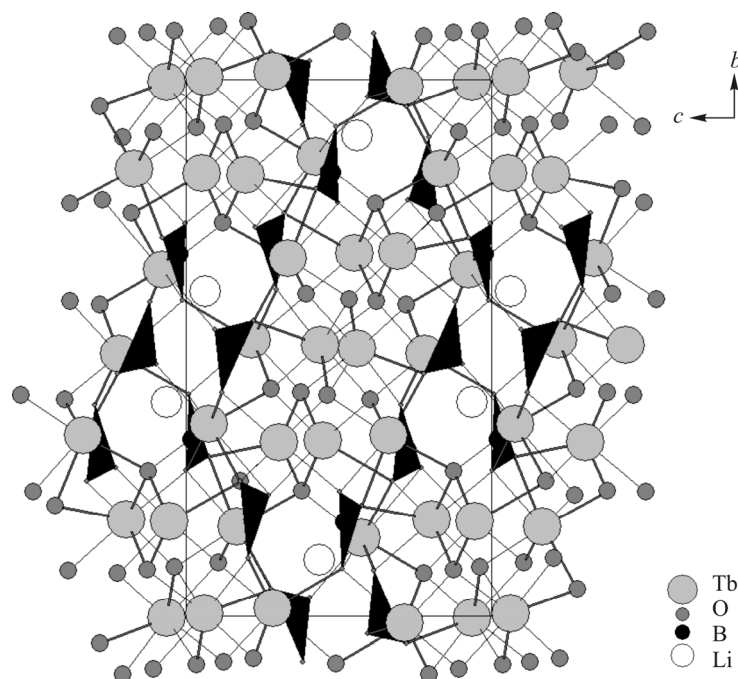

Fig. 3. Structure of the studied compound, view along axis *a*. The borate anions are shown by the polyhedral.

directed along the crystallographic axis *a* are formed. Triangular borate anions are located along the channel walls, while lithium ions occur inside the channels (Fig. 3).

The nearest environment of the lithium atom contains seven oxygen atoms from borate anions; the average Li–O distance is 2.32 Å.

The structure of the studied $LiTb_6O_5(BO_3)_3$ compound is very similar to the one previously published for $LiGd_6O_5(BO_3)_3$ [9]. The similarity of these structures is revealed by superimposing them on each other (after transforming the coordinates of $LiTb_6O_5(BO_3)_3$ from $P2_1/n$ to $P2_1/c$). Even though the idea of using the $LiGd_6O_5(BO_3)_3$ model [9] as the basis to solve the structure was not successful, it allowed finding the positions of "light" atoms when applied to the heavy cationic part of the system. Thus, both structures can be converted to fluorite-type, the predecessor of this structural series. The matrices describing the transition from fluorite to $LiTb_6O_5(BO_3)_3$ and to $LiGd_6O_5(BO_3)_3$ are

$$
\begin{array}{ccc}
3/2 & 0 & 1/2 \\
0 & 3 & 0 \\
-1/2 & 0 & 3/2
\end{array}
\quad \text{and} \quad
\begin{array}{ccc}
3/2 & 0 & -1/2 \\
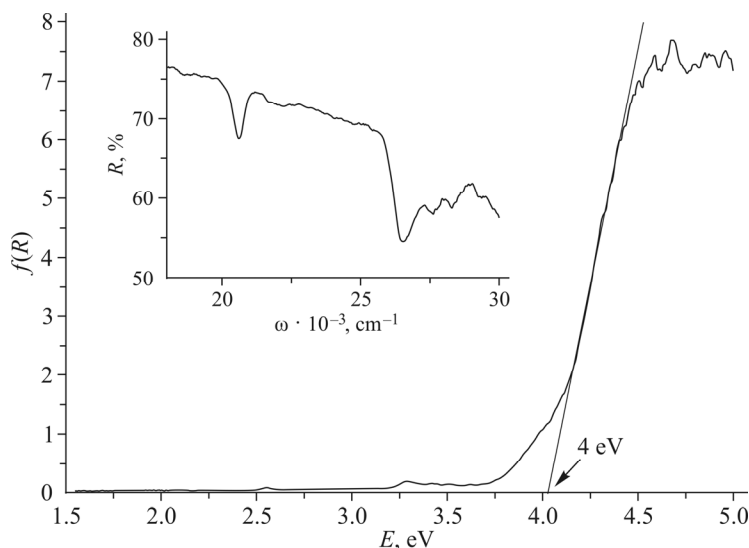0 & 3 & 0 \\
-1 & 0 & 2
\end{array}
\quad \text{, respectively.}
$$

Fig. 4. Diffuse reflectance spectrum of $LiTb_6O_5(BO_3)_3$ plotted in Kubelka–Munk units $F(R) = (1 - R)^2/2R$, where R is the reflectance coefficient. The inset shows the same spectrum in $\omega(cm^{-1})$–reflectance coefficient(%) coordinates in the region of 17500-30000 cm^{-1} demonstrating the f–f transitions of Tb^{+3} ions.

The cationic part of the predecessor's structural type is filled by cations RE^{3+} and Li^+, while the anionic part is filled by the oxygen atoms of oxide ions (O10–O14) and borate anions (O1–O9). The structure is distorted due to the difference between the radii of RE^{3+} and Li^+ and due to the bonds inside $(BO_3)^{3-}$. The determinant of both matrices is 7.5, i.e. the idealized fluorite cell is enlarged by 7.5 times.

The band gap was estimated using the diffuse reflectance spectrum in the Kubelka–Munk representation and was found to be 4 eV (Fig. 4). This value slightly exceeds the value of 3.74 eV reported earlier for Tb_2O_3 [28]. The spectrum of the sample also contains individual narrow absorption bands in the near UV and in the blue regions corresponding to the f–f transitions of trivalent terbium ions: 28300 cm^{-1} for $^7F_6 \rightarrow {}^5D_2$, 27600 cm^{-1} for $^7F_6 \rightarrow {}^5L_{10}$, 26500 cm^{-1} for $^7F_6 \rightarrow {}^5D_3$, 20600 cm^{-1} for $^7F_6 \rightarrow {}^5D_4$ (Fig. 4, inset), in agreement with [29].

Thus, the developed methods allow preparing $LiTb_6O_5(BO_3)_3$ both in the form of powder and in the form of millimeter size single crystals. The structure of this compound was determined, its similarity with $LiGd_6O_5(BO_3)_3$ and with fluorite (the predecessor of the series) was revealed. The band gap and the melting point were determined.

ACKNOWLEDGMENTS

FUNDING

CONFLICT OF INTERESTS

The authors declare that they have no conflict of interests.

REFERENCES

1. E. A. Khazanov. *Phys. Usp.*, **2016**, *59*, 886, DOI: 10.3367/UFNe.2016.03.037829.

2. C. T. Chen, Y. C. Wu, and R. K. Li. *Int. Rev. Phys. Chem.*, **1989**, *8*, 65, DOI: 10.1080/01442358909353223.

3. D. A. Keszler. *Curr. Opin. Solid State Mater. Sci.*, **1996**, *1*, 204, DOI: 10.1016/s1359-0286(96)80085-4.

4. P. Becker. *Adv. Mater.*, **1998**, *10*, 979, DOI: 10.1002/(SICI)1521-4095(199809)10:13<979::AID-ADMA979>3.0.CO;2-N.

5. J. P. Chaminade, O. Viraphong, F. Guillen, C. Fouassier, and B. Czirr. *IEEE Trans. Nucl. Sci.*, **2001**, *48*, 1158, DOI: 10.1109/23.958742.

6. D. M. Slaughter, C. R. Stuart, R. F. Klaass, and D. B. Merrill. *IEEE Trans. Nucl. Sci.*, **2016**, *63*, 1650, DOI: 10.1109/TNS.2016.2561240.

7. J. Y. Zhang, J. Yin, Y. Jiang, F. Du, S. K. Pan, X. Li, and J. G. Pan. Radiat. Meas., **2019**, *124*, 132, DOI: 10.1016/j.radmeas.2019.04.008.

8. Y. C. Lin, M. Karlsson, and M. Bettinelli. *Top. Curr. Chem.*, **2016**, *374*, DOI: 10.1007/s41061-016-0023-5.

9. J. P. Chaminade, P. Gravereau, V. Jubera, and C. Fouassier. *J. Solid State Chem.*, **1999**, *146*, 189, DOI: 10.1006/jssc.1999.8331.

10. J. H. Gao. *Chin. J. Struct. Chem.*, **2006**, *25*, 1175.

11. V. Jubera, P. Gravereau, J. P. Chaminade, and C. Fouassier. *J. Solid State Chem.*, **2001**, *156*, 161, DOI: 10.1006/jssc.2000.8977.

12. P. Gravereau, J. P. Chaminade, S. Pechev, V. Nikolov, D. Ivanova, and P. Peshev. *Solid State Sci.*, **2002**, *4*, 993, DOI: 10.1016/S1293-2558(02)01344-4.

13. G.-C. Zhang, P.-Z. Fu, Y.-G. Li, and Y.-C. Wu. *J. Synth. Cryst.*, **2005**, 765.

14. P. Peshev, S. Pechev, V. Nikolov, P. Gravereau, J. P. Chaminade, D. Binev, and D. Ivanova. *J. Solid State Chem.*, **2006**, *179*, 2834, DOI: 10.1016/j.jssc.2006.01.027.

15. G. Corbel, M. Leblanc, E. Antic-Fidencev, and M. Lemaitre-Blaise. *J. Solid State Chem.*, **1999**, *144*, 35, DOI: 10.1006/jssc.1998.8107.

16. G. Heymann, K. Beyer, and H. Huppertz. *Z. Naturforsch. Sect. B*, **2004**, *59*, 1200.

17. Q. D. Zeng and R. K. Li. *Solid State Sci.*, **2010**, *12*, 2144, DOI: 10.1016/j.solidstatesciences.2010.09.013.

18. P. Y. Chen, M. M. Murshed, and T. M. Gesing. *SN Appl. Sci.*, **2020**, *2*, DOI: 10.1007/s42452-020-2553-2.

19. V. Jubera, P. Veber, M. Chavoutier, A. Garcia, F. Adamietz, V. Rodriguez, J. P. Chaminade, and M. Velazquez. *Crystengcomm*, **2010**, *12*, 355, DOI: 10.1039/b912819k.

20. V. Jubera, J. Sablayrolles, F. Guillen, R. Decourt, M. Couzi, and A. Garcia. *Opt. Commun.*, **2009**, *282*, 53, DOI: 10.1016/j.optcom.2008.09.075.

21. J. P. Chaminade, V. Jubera, A. Garcia, P. Gravereau, and C. Fouassier. *J. Optoelectron. Adv. Mater.*, **2000**, *2*, 451.

22. V. Jubera, J. P. Chaminade, A. Garcia, F. Guillen, and C. Fouassier. *J. Lumin.*, **2003**, *101*, 1, DOI: 10.1016/S0022-2313(02)00335-6.

23. V. Jubera, A. Garcia, J. P. Chaminade, F. Guillen, J. Sablayrolles, and C. Fouassier. *J. Lumin.*, **2007**, *124*, 10, DOI: 10.1016/j.jlumin.2006.01.355.

24. Q. Wen, Z. F. Xiang, X. J. Gao, X. L. Yang, and S. G. Xiao. *Mater. Sci. Eng. B*, **2015**, *197*, 82, DOI: 10.1016/j.mseb.2015.01.010.

25. M. Kalidasan, R. A. Kumar, K. Asokan, and R. Dhanasekaran. *Nucl. Instrum. Methods Phys. Res.*, *Sect. B*, **2012**, *280*, 134, DOI: 10.1016/j.nimb.2012.03.002.

26. Y. I. Gibner and I. G. Vasilyeva. *J. Therm. Anal. Calorim.*, **1998**, *53*, 151, DOI: 10.1023/A:1010115620439.

27. G. M. Sheldrick. *Acta Crystallogr.*, *Sect. A*, **2015**, *71*, 3, DOI: 10.1107/S2053273314026370.

28. F. Vratny. *J. Chem. Phys.*, **1961**, *34*, 1377, DOI: 10.1063/1.1731747.

29. A. Y. Freidzon, I. A. Kurbatov, and V. I. Vovna. *Phys. Chem. Chem. Phys.*, **2018**, *20*, 14564, DOI: 10.1039/c7cp08366a.